www.ietdl.org

Published in IET Image Processing
Received on 22nd September 2011
Revised on 11th March 2012
doi: 10.1049/iet-ipr.2011.0459

ISSN 1751-9659

Kolmogorov superposition theorem for image compression

P.-E. Leni Y.D. Fougerolle F. Truchetet

LE2I Laboratory, UMR CNRS 6306, University of Burgundy IUT Le Creusot, 12 rue de la fonderie, 71200 LE CREUSOT, France
E-mail: pierre-emmanuel.leni@u-bourgogne.fr

Abstract: The authors present a novel approach for image compression based on an unconventional representation of images. The proposed approach is different from most of the existing techniques in the literature because the compression is not directly performed on the image pixels, but is rather applied to an equivalent monovariate representation of the wavelet-transformed image. More precisely, the authors have considered an adaptation of Kolmogorov superposition theorem proposed by Igelnik and known as the Kolmogorov spline network (KSN), in which the image is approximated by sums and compositions of specific monovariate functions. Using this representation, the authors trade the local connectivity and the traditional line-per-line scanning, in exchange of a more adaptable and univariate representation of images, which allows to tackle the compression tasks in a fundamentally different representation. The contributions lie in the several strategies presented to adapt the KSN algorithm, including the monovariate construction, various simplification strategies, the proposal of a more suitable representation of the original image using wavelets and the integration of this scheme as an additional layer in the JPEG 2000 compression engine, illustrated for numerous images at different bit rates.

1 Introduction

Compression has become a very familiar tool of our digital everyday lifes through widely used formats and standards for music, video and image, such as mp3, jpg, zip etc. Compression aims at the reduction of the redundancy of data and can be lossy or lossless. Lossless compression is often preferred to lossy compression for archival of high-quality images, such as medical images, technical drawings, clip arts and comics, because lossy compression methods introduce artefacts when used at low bit rates. Nevertheless, lossy methods are appropriate for the compression of natural images, for which a substantial bit rate reduction can be obtained in exchange of minor loss of fidelity. Image compression has been intensely studied for the past decades, and has led to various techniques and standards, including for the lossless compressions: the run-length encoding (used as default method in PCX and possibly in BMP, TGA or TIFF), differential pulse code modulation (DPCM) and predictive coding, entropy encoding, adaptive dictionary algorithms such as Lempel-Ziv-Welch (LZW) (used in GIF and TIFF), deflation (used in PNG, MNG and TIFF) [1] or chain codes [2]. The lossy compression techniques include the reduction of the colour space [3], chroma subsampling [4], fractal compression [5] and transform coding, which is the most commonly used method.

The method we propose in this paper is derived from the theoretical aspects of the Kolmogorov superposition theorem (KST), belongs to the lossy compression techniques and is characterised by two distinct contributions. The first original feature of our approach concerns the approximation of the original image (seen as a subsample of a continuous bidimensional function), as sums and compositions of mono-dimensional specific and continuous functions called internal and external functions. Such representation can be interpreted as an exchange of the local connectivity of the pixels and the traditional line-per-line scanning for a monovariate and more flexible representation with adjustable scanning direction, which allows for the application of simpler one-dimensional (1D) compression techniques. The second characteristic lies in the combination of several techniques to improve the compression results, even at low-bit rates. More specifically, our approach combines wavelet transform, function simplification and interpolation using the continuity of the representation, and the integration of the complete scheme as an additional step in the JPEG 2000 compression engine.

The KST is the solution to one of the 23 mathematical problems conjectured by Hilbert in 1900, who suggested that solutions to high-order equations were at least bivariate functions. This hypothesis was proven wrong by Kolmogorov in 1957, who showed that continuous multivariate functions can be expressed as sums and compositions of monovariate functions [25]. Unfortunately, such fundamental existence theorem has not been immediately applied, and some authors even suggested it was irrelevant [6]. Between the introduction of the theorem and the late 90s, most of the research efforts have been put into the definition and the construction of the monovariate

functions. Hecht-Nielsen, in [7], identified the analogy between the KST and double-layer neural networks. The first and most notable contribution to the monovariate functions construction is due to Sprecher [8] and [9], who proposed an explicit and exact algorithm, which first raised attention onto the possible applications of KST. We have implemented this algorithm, using the improvements proposed in [10], and applied on image decomposition in [11]. An equivalent approach built upon Sprecher's work and aiming at image processing has also been proposed by Köppen in [12, 13].

Sprecher's algorithm is characterised by the fact that the monovariate functions can be computed for any coordinates of the definition space at a given accuracy. Unfortunately, no analytic expression of the monovariate function is provided. Most importantly, the definition and the construction of the monovariate functions cannot be modified without completely modifying the overall construction scheme of this method. Precisely, the computation of the internal and external functions is fixed and depends on the number of digits considered, as well as the fixed number of layers depends on the dimension of the space.

Most of these issues have been overcome by Igelnik *et al.* in [14, 15] with the Kolmogorov spline network (KSN). In exchange of the accuracy of Sprecher's algorithm, the KSN approximates the monovariate functions and offers flexibility on several parameters of the algorithm. The KSN algorithm allows one to adjust the parameters used for the monovariate construction (tile size, sample points, sweeping orientation etc) and the number of layers, as explained in Section 2. Such flexibility is not obtained by increasing the overall complexity of the computations as shown in [11]: both techniques have equivalent complexity. One of the key aspect of our method is that the network can be modified to contain only a fraction of the pixels of the whole image (the smaller the tiles, the larger the quantity of information). Unfortunately, a slight increase of the tile size results in a strong quality decrease. Therefore to improve the reconstruction quality, we have combined KSN and wavelets: owing to their sparsity, the detail images can be reconstructed from a larger tilage decomposition for an equivalent image quality, which implies that the corresponding external functions can be more efficiently simplified to reduce the number of coefficients retained for the network construction, as we have proposed in preliminary previous approaches in [16].

We present several results of our complete compression scheme. We illustrate the strength of our approach through its integration within the JPEG 2000 engine. As illustrated in the rest of the paper, the results obtained compared to original JPEG 2000 are favourable to our method, which illustrates that our approach can be used to improve existing efficient compression techniques. Our contributions include improvements of the KSN algorithm for image decomposition, the analysis of the reconstruction quality, its combination with wavelet decomposition and its integration as an additional step into JPEG 2000, as illustrated on several examples at different bit rates.

The structure of the paper is as follows. The modified KSN algorithm is detailed in Section 2. In Section 3, the results of the grey-level image decompositions are presented; we combine the KST decomposition with wavelets to improve the reconstruction, and JPEG 2000 integration is described. In the last section, we present our conclusions and several promising research perspectives.

2 Algorithm

The KST, as reformulated and simplified by Sprecher in [17], can be written as

Theorem 1 (The KST): Every continuous function defined on the identity hypercube, $f:[0, 1]^d \to \mathbb{R}$, can be written as sums and compositions of continuous monovariate functions as

$$\begin{cases} f(x_1, \ldots, x_d) = \sum_{n=0}^{2d} g_n(\xi(x_1 + bn, \ldots, x_d + bn)) \\ \xi(x_1 + bn, \ldots, x_d + bn) = \sum_{i=1}^{d} \lambda_i \psi(x_i + bn) \end{cases} \quad (1)$$

with ψ and g_n as continuous monovariate functions, λ_i and b as constants. ψ is called an internal function and g_n are external functions. Co-ordinates x_i, $i \in 1, d$ are combined into a real number by a hash function ξ (obtained by linear combinations of internal functions ψ), which is associated with the corresponding value of f for these coordinates by the external functions g_n. A fundamental property of this approach is that the functions ξ and ψ are independent of the function f. The number of layers is constant and is a function of the dimensionality of the function.

The algorithm for the construction of the corresponding monovariate functions is described in [8] and [9]. The lack of flexibility of Sprecher's algorithm has led us to consider Igelnik's algorithm. We present the original KSN structure, as attributed to Igelnik in [14, 15], which also contains the demonstrations of the algorithm's convergence. Using the KSN, the function f can be approximated as

$$\begin{cases} f(x_1, \ldots, x_d) \simeq \sum_{n=1}^{N} a_n g_n(\xi_n(x_1, \ldots, x_d)) \\ \xi_n(x_1, \ldots, x_d) = \sum_{i=1}^{d} \lambda_i \psi_{ni}(x_i) \end{cases} \quad (2)$$

Remark 1: In (1), one internal function ψ is defined for the whole network, and the argument x_i is translated by a constant b_n for each layer n. In Igelnik's algorithm, one internal function ψ_{ni} is defined per dimension (subscript i) and layer (subscript n).

2.1 Algorithm

We refer the interested reader to [16] for a detailed explanation of the algorithm. We briefly recall the construction steps and emphasise the construction of the external functions.

The first step of the monovariate function construction is the definition of a disjoint tilage over the definition space $[0, 1]^d$ of the multivariate function f. The tilage is constituted of disjoint hypercubes H_n (the tiles) obtained by the cartesian product of the disjoint intervals $I_n(j)$. We study bivariate functions, so the hypercubes H are squares; see Fig. 1*a*. The size of the tiles is the same for every layer, but the tilage is translated for every layer, thus ensuring that any point in [0, 1] is located on at least one interval I_n for $N - 1$ layers; see Fig. 1*b*.

For a given tilage layer n, d internal functions ψ_{ni} are generated (one per dimension) with randomly generated step heights to define an increasing step function. The values of the functions ψ_{ni} are interpolated by cubic splines [26]. The convex combination of these internal functions ψ_{ni} with real, linearly independent and strictly positive values λ_i is the

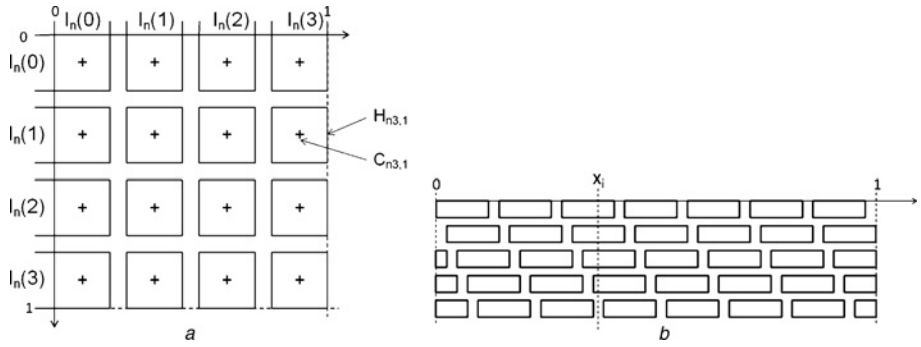

Fig. 1 *Detailed explanation of the algorithm*

a Cartesian product of disjoint intervals I_n to define a disjoint tilage of hypercubes H
b Superposition of translated disjoint tilages

argument of the external function g_n. Finally, the external function is constructed, using the a priori known values of the function f at the centres of the hypercubes. One couple of internal and external functions is associated with each tilage layer. We refer to the set constituted by all parameters defining all the internal and external monovariate functions as a network. To optimise the network construction, each layer is weighted by coefficients a_n. The flowchart of the complete network construction is presented in Figs. 2 and 3 presents an overview of a complete 5-tilage layer network.

2.2 Construction of the external functions g_n

One external function g_n is defined per tilage layer (of index n). First, a set of points $\mathcal{P}$ is computed. The abscissae of each point are the images of the associated function ξ_n, that is, real values $p_{nj_1,\ldots,j_d}$ that uniquely identify one hypercube $H_{nj_1,\ldots,j_d}$ from the tilage layer. The ordinates of each point are the images of the multivariate function f for the centres of the hypercubes $C_{nj_1,\ldots,j_d}$. For images decomposition, every ordinate corresponds to a pixel. Then, to obtain a continuous external function, the points of the set $\mathcal{P}$ are connected with 9° splines and straight lines.

The complex shape of the external function is related to the global sweeping scheme of the image: Sprecher and Draghici [18] demonstrated that sweeping curves can be defined using a mapping of the functions ξ_n. The linear combination of internal functions associates a unique real value with every d-tuple in the multidimensional space $[0, 1]^d$. Sorting these real values defines one unique path through the tiles of a

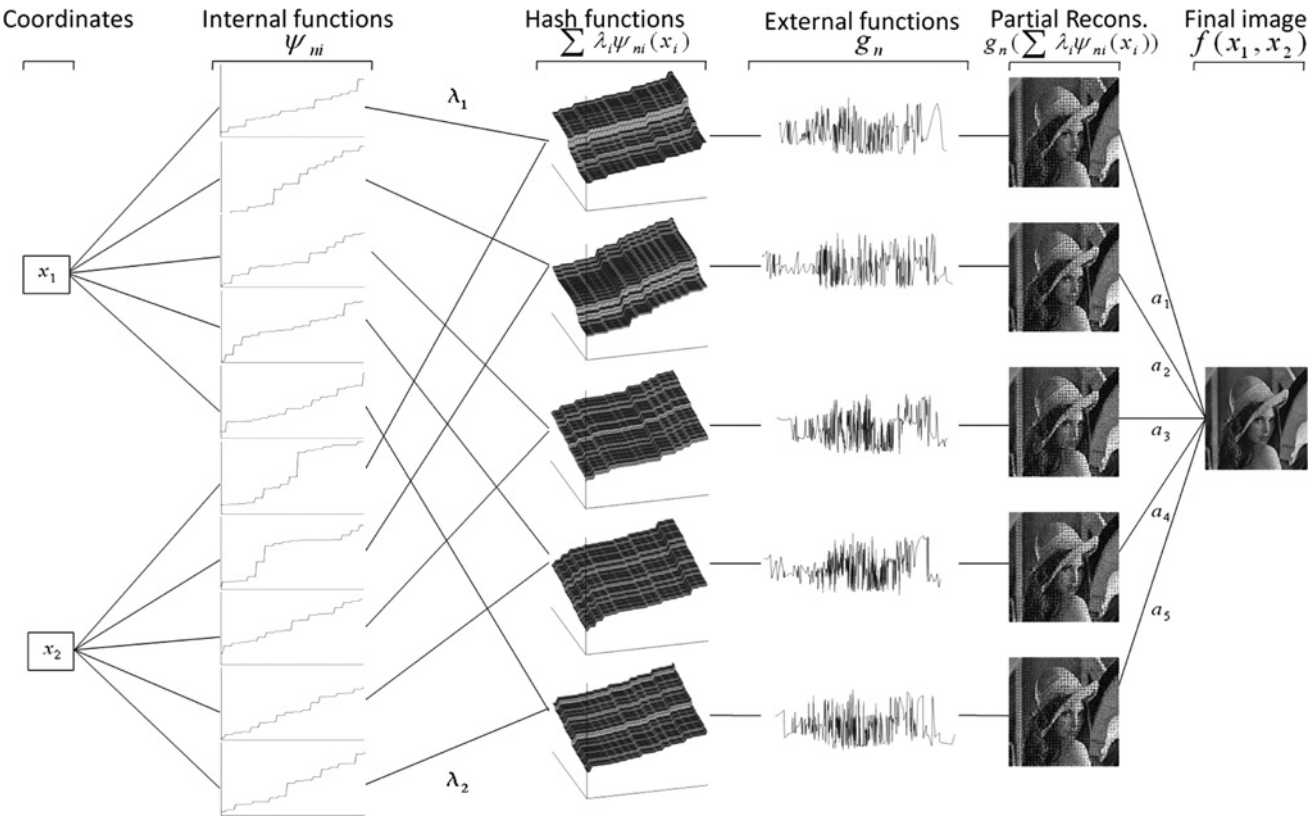

Fig. 2 *Overview of a 5-tilage layer network*

First step: to each coordinates x_i is associated one internal step function ψ per tilage layer
Second step: for a given layer, the internal functions are linearly combined to obtain the hash function ξ_n
Third step: the external functions are constructed using the images of the function ξ_n. Fourth step: the layers and weights a_n are linearly combined to reconstruct the image

doi: 10.1049/iet-ipr.2011.0459

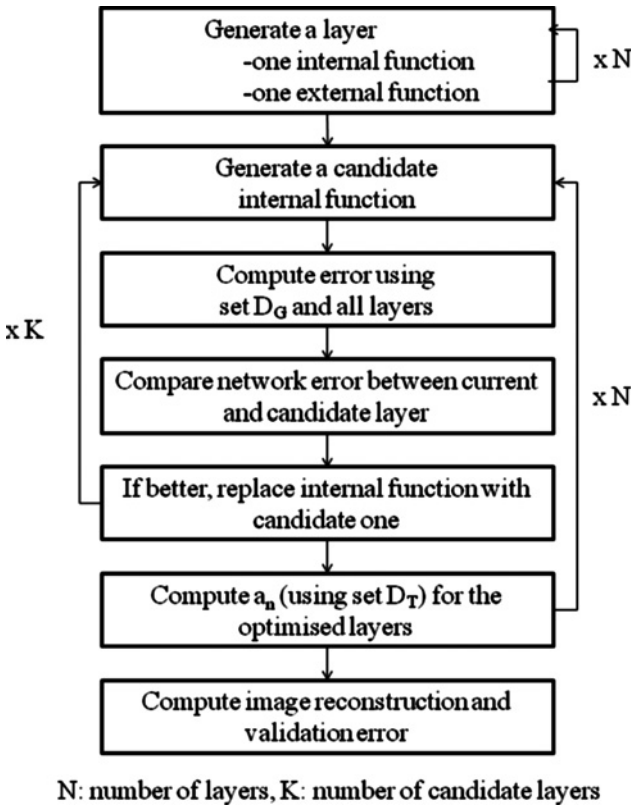

Fig. 3 *Network construction steps*

layer. Fig. 4 illustrates examples of such scanning curves, where the pixels are swept without any neighbourhood property conservation. Nevertheless, the global sweeping direction can be controlled using constants λ_1 and λ_2 used in (2). Fig. 4 presents three scanning functions using different constants λ_1 and λ_2, close to a diagonal sweeping, column-by-column sweeping and line-by-line sweeping.

From a practical point of view, the decomposition of a 200×200 image by a 10-tilage layer network with 120×120 tiles per layer requires about 2 min on an Intel i7 2.66 GHz. The decomposition consists in building several networks with various parameters, which can be done concurrently. The reconstruction consists in reading the values of the monovariate functions for a given (x_1, x_2) position, which is a straightforward operation, and requires only few seconds. Moreover, several positions can be retrieved simultaneously. Therefore as a perspective, the design of a hardware design to take advantage of the parallel encoding and decoding process can be considered.

3 Application to compression

3.1 Association of KSN and wavelets for image compression

We present several strategies to reduce the information required to build the internal and the external functions. Images can be seen as bivariate functions in which each pixel corresponds to a tile of the bidimensional space $[0, 1]^2$ over which bivariate function is constant. By changing the parameters δ and N, the size of the tilage can be adjusted, that is, the number of tiles per layer. The tile size directly determines the number of pixels that are used for the network construction, because the pixel values are utilised to construct the external functions g_n. In terms of transmission, a compression is realised, since the quantity of pixels needed to reconstruct the original image is decreased. Nevertheless, the reconstruction quality rapidly decreases and artefacts are visible and are due to the approximation errors between the tiles.

To improve the overall reconstruction quality, we combine the KSN with wavelet approaches. The interested reader can find a complete wavelet introduction in [19]. We used a separable wavelet basis to filter the lines and the columns of the image separately. The image is split into four sub-images, with one sub-image containing the low frequencies and three containing the high frequencies. Our goal is to decompose the detail images (high-frequency images) using small tiles, and, taking advantage of the limited contrast and the sparse representation, to reduce the number of coefficients from the original detail images required for the construction of the external functions as if larger tiles were used. Moreover, to optimise the decomposition, the global sweeping scheme is controlled by adjusting the constants λ_1 and λ_2 to match the orientations of the detail images, as illustrated on Fig. 4: line-by-line sweeping (c) for the horizontal details, column-by-column (b) for vertical details

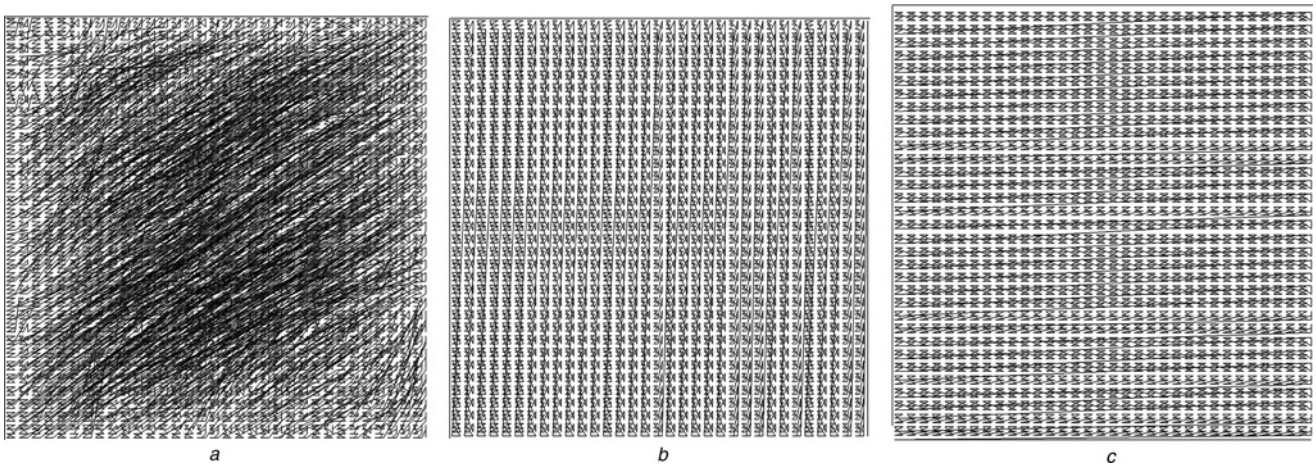

Fig. 4 *Examples of sweeping curves*

a With $\lambda_1 \simeq 0.55$ and $\lambda_2 = 0.4$
b With $\lambda_1 \simeq 0.95$ and $\lambda_2 = 0.00004$
c With $\lambda_1 = 0.00004$ and $\lambda_2 \simeq 0.95$

and diagonal (a) for diagonal details. An interesting property is that the decomposition of the detail images leads to external functions that can be simplified using two approaches, which are both applied during the construction of the external functions. The first step is the generation of points of the set $\mathcal{P}$ (see Sections 2 and 2.2), and then, the simplifications are applied to decrease the number of pixels retained for the network construction. In other words, by simplifying the external functions, the cardinal of the set $\mathcal{P}$ is decreased, so as the number of coefficients retained to build the network.

The first simplification uses the mean value. For each external function g_n with mean μ_n and standard deviation σ_n, the number of pixels retained for network construction can be decreased by replacing values g_n by μ_n when

$$K \in \mathbb{N}^*, |g_n - \mu_n| < \frac{\sigma_n}{K} \tag{3}$$

The constant K can be adjusted: the smaller, the greater the number of simplified values. With this method, some of the pixels located at the centres of the hypercubes are no longer required, as illustrated in Figs. 5*a* and *b*. In this paper, we consider only natural images with similar complexity. Therefore the images of details tend to have a similar distribution of coefficients, and K does not need to be adjusted for every image. Nevertheless, when considering images of various complexities, K has to be determined for each image, to remove enough wavelet coefficients such that the remaining ones fit in a given number of sub-bands.

The second simplification takes advantage of the external function continuity. Some values in the external functions can be simplified and approximated by linear interpolation. Precisely, for each point of abscissa t_0, the slopes of two lines are computed, one connecting the previous point (of abscissa t_{-1}): $r_0 = \{[g(t_0) - g(t_{-1})]/(t_0 - t_{-1})\}$, and one connecting the next point (of abscissa t_1): $r_1 = \{[g(t_1) - g(t_0)]/(t_1 - t_0)\}$. The points of abscissa t_0 can be removed if aligned with the points of abscissa t_{-1} and t_1

$$\varepsilon \in \mathbb{R}, \frac{r_0}{r_1} = 1 \pm \varepsilon \tag{4}$$

The constant ε can be adjusted: the bigger, the greater the number of simplified values. The points verifying the alignment criterion can be removed and linearly interpolated (dashed-line), as illustrated in Fig. 5*c*.

The combination of the KSN decomposition with wavelets systematically outperforms bicubic and nearest neighbour interpolations, even at high-compression rates, peak signal-to-noise ratio (PSNR) is systematically higher, as shown in [16] and [20]. Fig. 6 presents the results obtained with medium and high simplification criteria for external function simplifications. We observe that the reconstruction

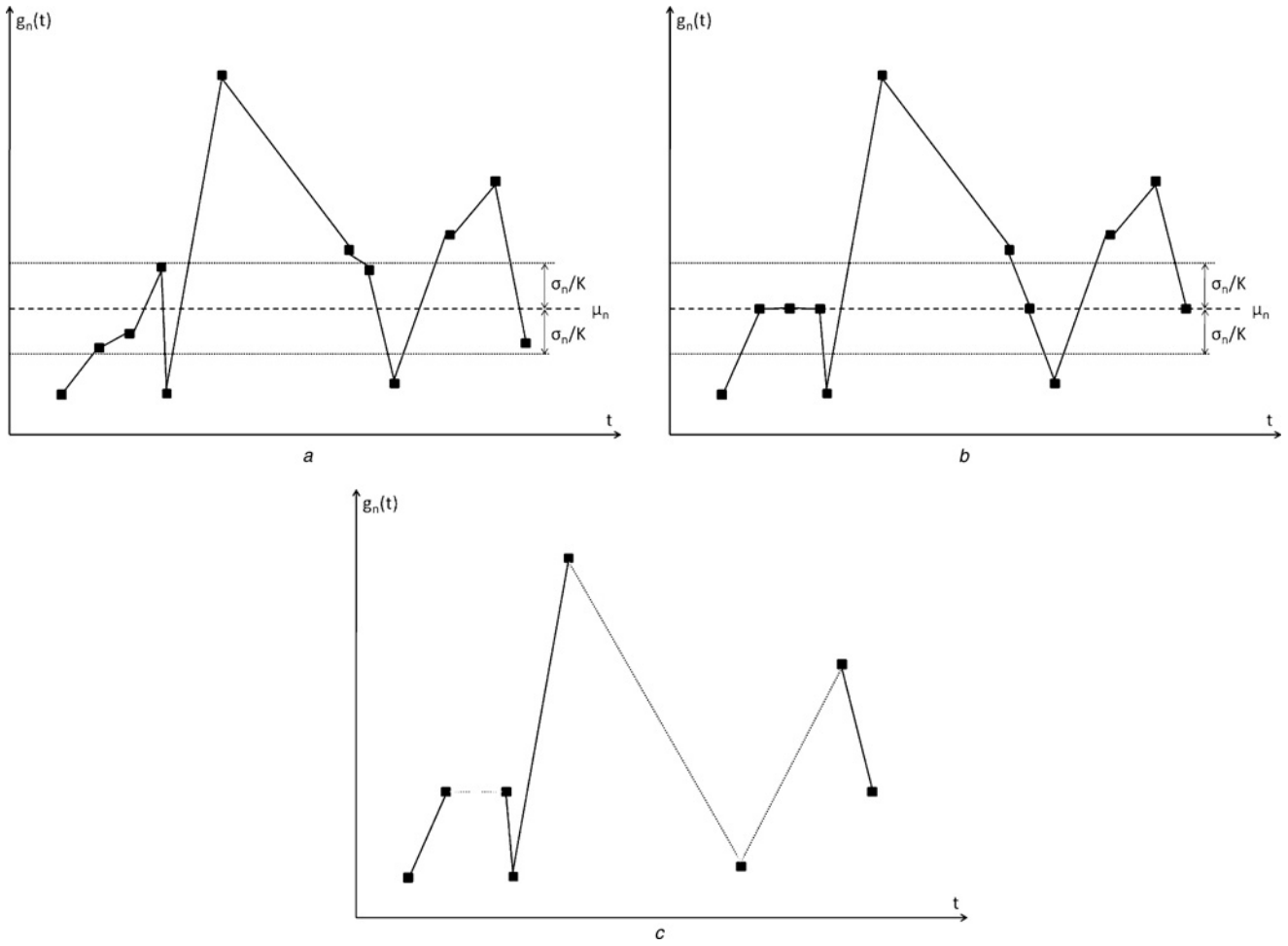

Fig. 5 *External function simplifications*

a Original function
b Mean simplification
c Linearity simplification

doi: 10.1049/iet-ipr.2011.0459

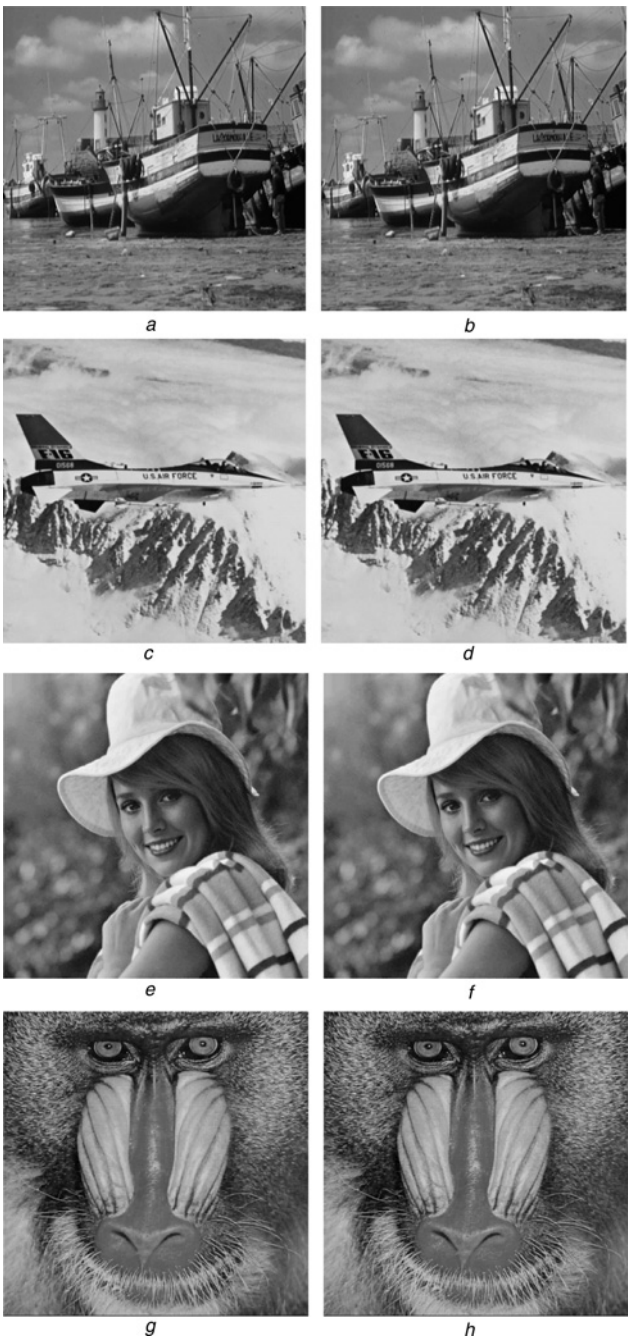

Fig. 6 *Reconstructions of*
a and *b* Boat
c and *d* F16
e and *f* Elaine
g and *h* Mandrill
using about 45 and 65%, respectively, of the original wavelet coefficients

is not visibly altered, even when only 45% of the original wavelet coefficients are retained.

3.2 Compression efficiency

We first detail the influence of the monovariate function simplifications on the decomposed detail images. Table 1 presents the entropy of a simplified sub-band (with removed coefficients) and original sub-band for Lena, Peppers and Mandrill, respectively. We observe that the entropy is slightly lower than the original sub-band for simplification with $K = 4$ (defined in 3), which corresponds to a good compromise between simplifications and reconstruction quality: the number of coefficients to encode decreases, whereas the redundancy between values is greatly reduced. Finally, there are less, but all different, coefficients. With the highest possible simplification, $K = 2$, the entropy is decreased as well as the number of coefficients, but this simplification is too destructive to be useful. Finally, we can note that the complexity of the content of an image slightly modify the simplification that can be achieved: for an image with smooth content (Peppers), the entropy obtained with $K = 4$ is around 88% of its original value, and on more complex images (Lena and Mandrill, respectively), it is decreased to 86 and 83% of its original value. Similarly, with $K = 2$, it is decreased to 58% of the original value for Peppers, and to 60 and 61% for Lena and Mandrill.

To illustrate the influence of the decomposition into monovariate functions, we measure the entropy of the external functions. We assume that the external functions are encoded using a vector quantisation and we simulate the encoding of the points remaining after the mean and linearity simplifications. For comparison, we sweep line-by-line the original sub-band and encode the obtained 1D signal using the same method. We also sweep line-by-line the remaining coefficients after removing 50% of the coefficients using a cubic interpolation. Table 2 presents the obtained entropies. One can see that the mean entropy per vector is higher for an external function, but the total number of bits to encode the whole function is lower than with other approaches, because the number of vectors to be encoded is lower. In other words, the simplifications performed on the monovariate functions remove the redundancies, thus decrease the entropy by retaining only the critical coefficients. This 'smart' selection of the coefficients leads to better performances compared to classical interpolation methods.

3.3 Contribution to JPEG 2000

To compare with existing compression methods, we have integrated our method as a new step in the JPEG 2000 encoder and decoder (see [20]). We present new and detailed results, including two-level wavelet decomposition and comparison between the two types of wavelets used in JPEG 2000 (Le Gall 5–3 and Daubechies 9–7).

The JPEG 2000 standard supports lossy and lossless compression of single-component and multi-component images. Extra features can be mentioned, such as: progressive reconstruction by pixel accuracy or resolution, superior low–bit-rate performance than existing standards and good resilience to transmission errors. We briefly describe several steps in the JPEG 2000 algorithm, and we refer the interested reader to [21, 22], and [23] for details. The first step is the decomposition of the image into components, and optionally into tiles. Then, the wavelet transform is applied on each tile, at a different resolution levels. Two wavelet families can be applied: Le Gall 5–3 for reversible transform (lossless compression) and Daubechies 9–7 for irreversible transform (lossy compression). The decomposition levels are subdivided into sub-bands of coefficients (tiles), which are then quantised and converted into code blocks before being entropy encoded into bit planes. Lastly, the code stream is generated and a header is computed to describe various decomposition and coding parameters.

Table 1 Comparative measures of the entropy of a sub-band from Lena, before and after simplification

	Original			Simplified $K = 4$			Simplified $K = 2$		
	hh	hl	lh	hh	hl	lh	hh	hl	lh
Lena									
Entropy	3.44	4.14	3.69	2.99	3.43	3.30	2.14	2.18	2.44
Ratio	1	1	1	0.87	0.83	0.89	0.62	0.53	0.66
nb. of coef.	36 864	36 864	36 864	20 064	20 256	22 401	11 588	9868	13 301
Peppers									
Entropy	3.68	3.98	3.80	3.36	3.22	3.45	2.58	2.13	1.92
Ratio	1	1	1	0.91	0.81	0.91	0.70	0.53	0.50
nb. of coef.	36 864	36 864	36 864	24 980	19 644	24 159	15 922	10 323	9322
Mandrill									
Entropy	5.35	5.40	5.94	4.59	4.53	4.68	3.45	3.39	3.40
Ratio	1	1	1	0.86	0.84	0.79	0.64	0.63	0.57
nb. of coef.	36 864	36 864	36 864	24 894	24 477	22 125	16 437	16 036	14 252

Table 2 Comparative measures of the entropy of a sub-band encoded by vector quantisation

	Line-by-line	Cubic interp.	KSN ext. func.
Req. vectors	2129	1290	314
Mean entropy	2.43	3.09	3.00
Std. deviation	0.51	0.30	0.27
Total entropy	5182	3986	943

We add an additional layer between wavelet transformation and quantisation, in which the KSN decomposition scheme is used to simplify the wavelet coefficients (as in Sections 3 and 3.1), without further modifications in the encoding scheme. Fig. 7 presents the modified JPEG 2000 engine. After decomposition and simplification, we obtain a detail image with 'holes' where some coefficients can be ignored; see Fig. 8*a*. Such an 'image' cannot be directly computed by JPEG 2000, which requires values for every pixel. We modify the organisation of coefficients to decrease the size of the detail images, thus decreasing the number of sub-bands. In other words, the detail images are decomposed into blocks of coefficients before further encoding steps; by reorganising the coefficients after simplification, the quantity of blocks required to encode the detail images can be decreased. The coefficients are formatted to be fully contained in the several blocks that are computed after quantisation and before bit-plane coding, which reduces the size of the images by coding only a limited number of blocks. To do so, a binary table of same size as the sub-bands is utilised to memorise if a pixel has been simplified. The remaining coefficients are read line-by-line to obtain a 1D representation (see Fig. 8*b*) and then reorganised to fill the image block-per-block (see Fig. 8*c*). This rearrangement, imposed by JPEG 2000 scheme, is used only for exploratory approach and is not optimal: the JPEG 2000 encoder is not optimised to take advantage of uncorrelated coefficients, such as the one obtained after simplification and rearrangement.

Fig. 9 presents the results of a JPEG 2000 compression of a 384×384 pixel image, with and without additional KSN step for LeGall 5–3 wavelets (Fig. 9*a*) and Daubechies 9–7 wavelets (Fig. 9*b*). For our experiments, we limit to one-level and two-level wavelet decompositions, and decrease the size of block coefficients from 64×64 to 32×32. Below 1 bpp bit rate and with only one decomposition level, the reconstruction PSNR of the original JPEG 2000 and our approach rapidly decreases: to achieve such bit rates with only one level, there is no other choice than almost simplify all the coefficients in the detail images. In that case, the detail images contain almost only null coefficients, and our algorithm cannot reconstruct all coefficients that was simplified by JPEG 2000. This issue led us to increase the number of decomposition levels. With two-level decomposition, our approach still improves the PSNR, but the improvement remains marginal because some of the distortion introduced at the first decomposition

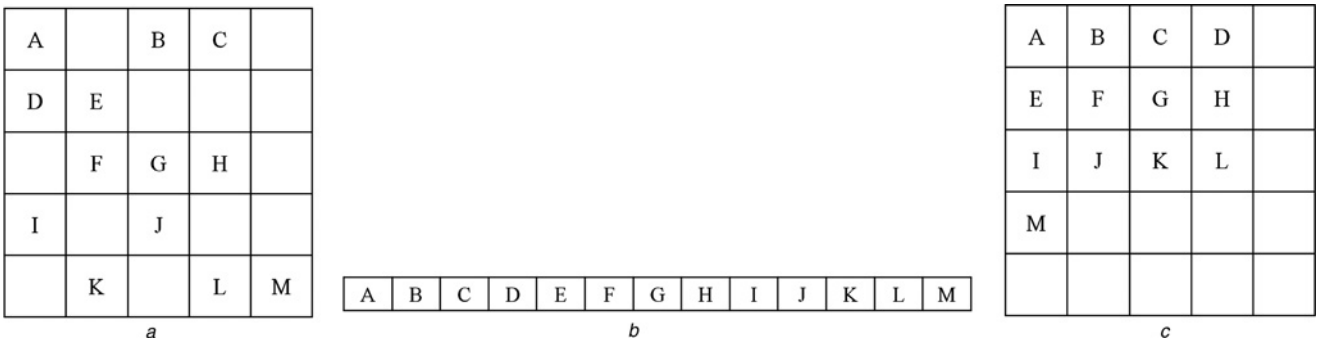

Fig. 7 *Detail image with 'holes' after decomposition and simplification*

a Detail image after simplification
b 1D representation
c 'Defragmented' detail image

doi: 10.1049/iet-ipr.2011.0459

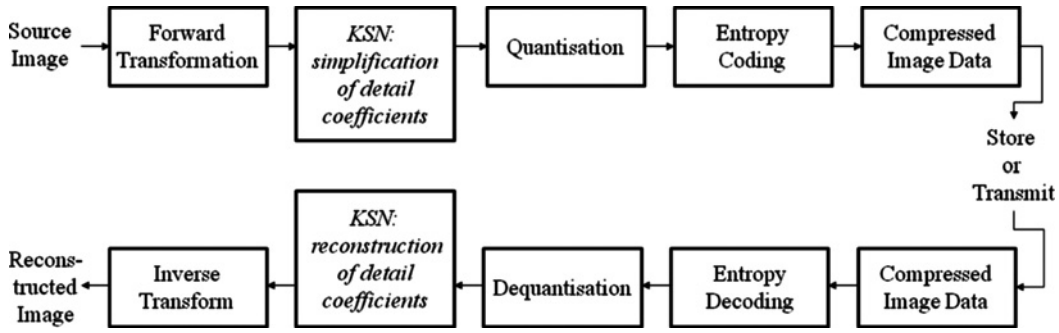

Fig. 8 *JPEG 2000 overview, including additional KSN decomposition*

level is spread to the next levels. The results show that the defragmentation of the wavelet coefficients before JPEG 2000 integration leads to better results. At higher bit rates, the minimum simplification already significantly reduces the image reconstruction accuracy, without simplifying enough coefficients to obtain a better compression performance than the original JPEG 2000: this is particularly noticeable on Fig. 9*a*, the point at 3.17 bpp corresponding to a result barely similar to JPEG 2000 without KSN decomposition.

The Tables 3 and 4 detail the compression ratio used in JPEG, the simplification parameters used for external functions, and the obtained PSNR at different bit rates. 'def' stands for the default compression ratios of JPEG 2000 (lossless compression when using LeGall 5–3

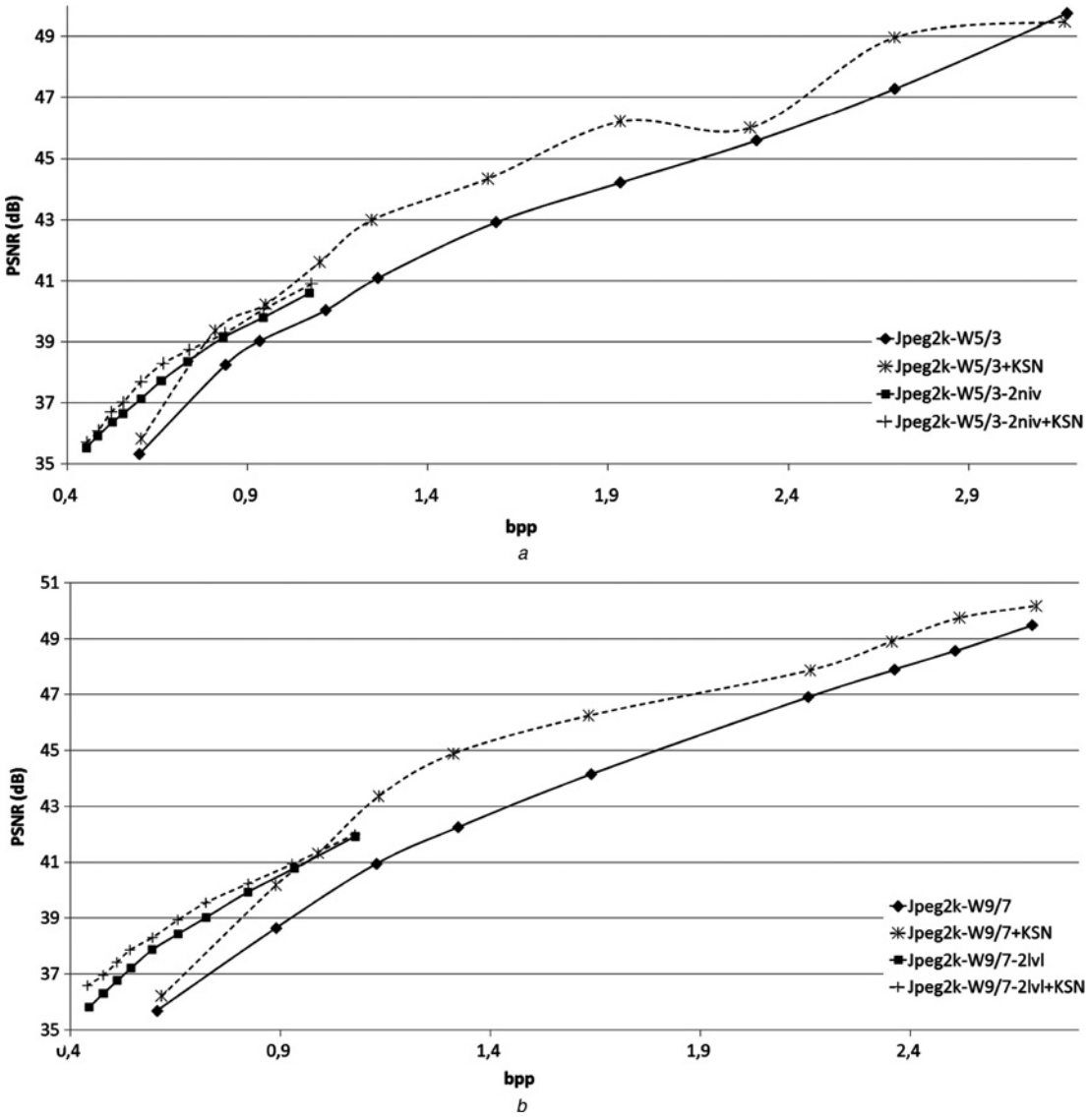

Fig. 9 *Comparison between JPEG 2000 with and without KSN*

a For LeGall 5–3 wavelets
b For Daubechies 9–7 wavelets

Table 3 PSNR of image reconstruction using LeGall 5–3 wavelets and KSN

Bit rate, bpp	JPEG ratio	K (mean value simplif.)	PSNR, dB
0.60	12	2	35.83
0.81	8	2	39.37
0.95	7	2	40.23
1.1	6	2	41.61
1.24	5	2	42.99
1.57	4	2	44.35
1.93	def	2	46.22
2.29	3	4	46.02
2.69	def[a]	4	48.97
3.17	def	6	49.49

[a]'def' stands for the default ratio of JPEG 2000 (that provides lossless compression).

Table 4 PSNR of image reconstruction using Daubechies 9–7 wavelets and KSN

Bit rate, bpp	JPEG ratio	K (mean value simplif.)	PSNR, dB
0.62	12	4 and 2	36.21
0.89	8	4 and 2	40.18
0.99	7	4 and 2	41.32
1.13	6	4 and 2	43.36
1.31	5	4 and 2	44.88
1.63	4	4 and 2	46.24
2.16	3	4 and 2	47.87
2.35	def[a]	4 and 2	48.90
2.52	def	4	49.74
2.7	def	6	50.17

[a]'def' stands for the default ratio of JPEG 2000 (that provides highest fidelity: coefficients are not modified through encoding).

wavelets and maximum accuracy with Daubechies 9–7 wavelets). Table 3 presents the results for LeGall 5–3 wavelets and Table 4 for Daubechies 9–7 wavelets. In Table 4, two different coefficients are used to simplify the external functions: diagonal and vertical details decompositions are simplified using $K = 4$ and horizontal details are simplified using $K = 2$. The goal is to obtain a similar number of coefficients for all the images of details, preserving a similar quality of reconstruction of horizontal, vertical and diagonal details. The simplification coefficient used with the LeGall 5–3 wavelets is $K = 2$, which leads to bit rates lower than 1.93 bpp. To obtain the intermediate result at 2.29 bpp, we used a simplification criterion $K = 4$ combined with a JPEG compression ratio, but this combination is less effective. The coefficient K and the JPEG 2000 compression ratio have to vary together. Little compression improvement is observed using high JPEG compression ratio with almost all coefficients (high value of K); and the reconstruction quality obtained with a low value of K and low compression ratio in JPEG 2000 is lower than when using only JPEG 2000.

Fig. 10 presents the reconstruction obtained with and without our additional decomposition and simplification step. It shows that the method does not add visible artefacts to JPEG 2000 compression and marginally improves the PSNR. Fig. 10*b* is obtained with a simplification of the external functions using $K = 2$. The remaining wavelet coefficients of detail images are reorganised and compressed using a ratio of five within JPEG 2000. Similarly, Fig. 10*d* is obtained with a simplification of the external functions using $K = 4$ for diagonal and vertical details, and $K = 2$ for horizontal details. The remaining coefficients are compressed with a ratio of five in JPEG 2000. Figs. 10*a* and *c* are obtained with minimum compression in JPEG 2000 and minimum simplifications.

Fig. 10 *Reconstruction obtained with and without our additional decomposition and simplification*

a and *b* Results with JPEG 2000 (LeGall 5–3 wavelets) and our method, at bit rates of 2.7 bpp and 1.3 bpp

c and *d* Results with JPEG 2000 (Daubechies 9–7 wavelets) and our method, at bit rates of 2.7 bpp and 1.3 bpp

4 Conclusion and perspectives

We have presented an adaptation of the KSN algorithm for image compression. We have shown that a modified KSN algorithm with adaptive tile size and modifiable sweeping direction, applied to wavelet representation of images, leads to efficient compression rates. Our algorithm benefits from the fact that, because of the sparse nature of detail images, a simplified representation of the external monovariate functions can be built while preserving the PSNR. The vertical, horizontal and diagonal detail images can be represented by external functions with corresponding scanning directions and adjusted tile sizes, which strongly increases the external function redundancy and allows for a better compression. We have illustrated our approach on several natural images and studied its behaviour at different bit rates for different simplification parameters. The integration within JPEG 2000 clearly illustrates an improvement of the compression rates, even if the gains remain limited because of the intermediate reorganisation, although necessary, of the data into blocks to assure the compatibility with JPEG 2000.

Several promising perspectives for the KSN representation of images can be pointed out. The implementation into JPEG 2000 remains experimental and may be improved. Actually, because our approach abandons the local connectivity of the pixels, any compression technique using representations by

doi: 10.1049/iet-ipr.2011.0459

blocks will dissipate part of the benefits, which leads to the development of fundamentally different compression algorithms. Another research perspective is currently dedicated to the decomposition scheme itself: the internal functions are required to rearrange the external functions to reconstruct the original image. One can imagine an encryption algorithm based on a key constituted by the internal functions, which could be used as a signature with applications to watermarking. A multiresolution approach has been investigated, in which the layers of a network have different tilage densities, which leads to an algorithm, in which the image is progressively reconstructed with increasing resolution by progressively superposing the layers [24]. Combining this progressive transmission approach with the encryption scheme using internal functions as a key could provide a novel approach for progressive transmission of encrypted images. The last and more challenging research perspectives are related to the statistical aspects of this method. For example, the noise resilience should be studied and may provide deeper insights into this approach. The KSN algorithm abandons the pixels organisation in exchange of a mono-dimensional and flexible representation: regarding the transmission of the external functions, any perturbation spreads within the reconstructed image, which limits the local distortions and reduce visible artefacts in the reconstructed image.

5 References

1 Salomon, D.: 'Data compression: the complete reference' (Springer-Verlag New York Inc, 2007)
2 Kui Liu, Y., Zalik, B.: 'An efficient chain code with Huffman coding', *Pattern Recognit.*, 2005, **38**, (4), pp. 553–557
3 Papamarkos, N., Atsalakis, A.E., Strouthopoulos, C.P.: 'Adaptive color reduction', *IEEE Trans. Syst. Man Cybern. B*, 2002, **32**, (1), pp. 44–56
4 Chen, H., Sun, M., Steinbach, E.: 'Compression of Bayer-pattern video sequences using adjusted chroma subsampling', *IEEE Trans. Circiuts Syst. Video Technol.*, 2009, **19**, (12), pp. 1891–1896
5 Barnsley, M.F., Hurd, L.P., Anson, L.F.: 'Fractal image compression' (AK Peters, Massachusetts, 1993)
6 Girosi, F., Poggio, T.: 'Representation properties of networks: Kolmogorov's theorem is irrelevant', *Neural Comput.*, 1989, **1**, (4), pp. 465–469
7 Hecht-Nielsen, R.: 'Kolmogorov's mapping neural network existence theorem'. Proc. IEEE Int. Conf. Neural Networks III, New York, 1987, pp. 11–13
8 Sprecher, D.A.: 'A numerical implementation of Kolmogorov's superpositions', *Neural Netw.*, 1996, **9**, (5), pp. 765–772
9 Sprecher, D.A.: 'A numerical implementation of Kolmogorov's superpositions II', *Neural Netw.*, 1997, **10**, (3), pp. 447–457
10 Braun, J., Griebel, M.: 'On a constructive proof of Kolmogorov's superposition theorem', *Constructive Approx.*, 2007, **30**, (3), pp. 653–675
11 Leni, P.-E., Fougerolle, Y.D., Truchetet, F.: 'Kolmogorov superposition theorem and its application to multivariate function decompositions and image representation'. Proc. IEEE Conf. Signal-Image Technology and Internet-Based System, IEEE Computer Society Washington, DC, USA, 2008, vol. 00, pp. 344–351
12 Köppen, M.: 'On the training of a Kolmogorov Network', Springer, Berlin, 2002, (*LNCS*, **2415**), pp. 140–145
13 Köppen, M., Yoshida, K.: 'Universal representation of image functions by the Sprecher construction', in Abrahim, A. (Ed.): 'Soft computing as transdisciplinary science and technology' (Springer, Berlin, 2005, vol. 29), pp. 202–210
14 Igelnik, B., Parikh, N.: 'Kolmogorov's spline network', *IEEE Trans. Neural Netw.*, 2003, **14**, (4), pp. 725–733
15 Igelnik, B.: 'Kolmogorov's spline complex network and adaptive dynamic modeling of data', in Nitta, T. (Ed.): *Complex-Valued Neural Netw. Utilizing High-Dimens. Parameters*, (Hershey, PA, 2009), pp. 56–78
16 Leni, P.-E., Fougerolle, Y.D., Truchetet, F.: 'Kolmogorov superposition theorem and wavelet decomposition for image compression', *Lect. Notes Comput. Sci.*, 2009, **5807**, pp. 43–53
17 Sprecher, D.A.: 'An improvement in the superposition theorem of Kolmogorov', *J. Math. Anal. Appl.*, 1972, **38**, pp. 208–213
18 Sprecher, D.A., Draghici, S.: 'Space-filling curves and Kolmogorov superposition-based neural networks', *Neural Netw.*, 2002, **15**, (1), pp. 57–67
19 Mallat, S.: 'A wavelet tour of signal processing' (Academic Press, San Diego, 1998)
20 Leni, P.-E., Fougerolle, Y.D., Truchetet, F.: 'The Kolmogorov spline network for image processing', in Igelnik, B. (Ed.): 'Computational modeling and simulation of intellect: current state and future perspectives' (IGI Global, 2011), pp. 25–51
21 Taubman, D., Marcellin, M.: 'JPEG2000, image compression fundamentals, standards and practice' (Kluwer Academic Publishers, 2001)
22 Skodras, A., Christopoulos, C., Ebrahimi, T.: 'The jpeg 2000 still image compression standard', *IEEE Signal Process. Mag.*, 2001, **18**, pp. 36–58
23 Adams, M.D.: 'The jpeg-2000 still image compression standard' (Technical Report, University of British Columbia, 2001)
24 Leni, P.-E., Fougerolle, Y.D., Truchetet, F.: 'New adaptive and progressive image transmission approach using function superpositions', *Opt. Eng.*, 2010, **49**, (9), pp. 097001–097011
25 Brattka, V.: 'Du 13-ième problème de Hilbert à la théorie des réseaux de neurones: aspects constructifs du théorème de superposition de Kolmogorov', in Charpertier, E., Lesne, A., Nikolshi, N. (Ed.): 'L'héritage de Kolmogorov en mathématiques' (Belin Editions, Paris, 2004), pp. 241–268
26 Moon, B.S.: 'An explicit solution for the cubic spline interpolation for functions of a single variable', *Appl. Math. Comput.*, 2001, **117**, pp. 251–255